J. Phys. Chem. A **1997,** *101,* 3855−3859

Study of Benzophenone Photolysis in SDS Micelles in the Presence of 2,4,6-Tri-*tert*-butylphenol: Distinctive Features of SNP in Radical Pairs with a Natural Abundance of ^{13}C Nuclei

Andrei P. Parnachev,[†] Elena G. Bagryanskaya,* and Renad Z. Sagdeev

International Tomography Center, Institutstakya st. 3a, 630090 Novosibirsk, Russia, and
Novosibirsk State University 630090 Novosibirsk, Russia

Received: May 28, 1996; In Final Form: September 24, 1996⊗

The ^{13}C-stimulated nuclear polarization (SNP) technique has been applied to study the photolysis of perdeuterated benzophenone in SDS micelles in the presence of 2,4,6-tri-*tert*-butylphenol with natural abundance of ^{13}C for both compounds. The relaxation rate constants have been determined for radical pairs differing in the position of the ^{13}C label, and the conclusions have been drawn regarding the pertinent relaxation mechanisms. The value of the exchange interaction in the radical pairs formed in the course of the reaction has been estimated, and the diminishing of the splitting in the SNP spectra has been observed. Distinctive features of SNP in systems with natural abundance of ^{13}C nuclei have been considered.

Introduction

Several techniques based on the indirect detection of magnetic resonance of radical intermediates, such as RYDMR[1] and PYESR,[2] became widely adopted in recent years. Stimulated nuclear polarization (SNP)[3] also belongs to this type of technique. The shapes of the experimentally obtained SNP spectra and kinetics are governed by the number and magnitude of HFI constants in the radical pairs (RP), the size and viscosity of a micelle, the rate constants of recombination and escape from the micelle into the bulk, the relaxation parameters, the magnitude of the electron spin exchange (ESE) interaction, and the amplitude of the microwave field B_1.

Of particular importance is the estimation of the ESE value, which plays an important role in RP recombination governing the rate of intersystem crossing (ISC). It also has a profound influence on the appearance of an SNP spectrum. A diminishing of the observed splitting in the SNP spectra due to high contact ESE value upon decreasing the micelle size has been observed in ref 4. This ESE effect is shown to be determined mainly by the ratio a/Z where a is the HFI constant and Z is the rate of forced re-encounters. If $a/Z \gg 1$, the splitting in the SNP spectra should be independent of ESE value and just equal to the HFI constant a, while in opposite case the ESE-induced diminishing of the splitting in SNP spectra should be observed.

In the recent work[4] the RPs comprising of benzyl and benzoyl radicals ^{13}C labeled in carbonyl group ($a = 12.7$ mT) were studied in micelles of different size. There the value a/Z was varied, and significant diminishing of the splitting in the SNP spectra was observed with the decrease of the micelle size. On the other hand, for RPs investigated in ref 5 ($a = 37.8$ mT), the splitting in SNP spectra turns out to be essentially independent of the micelle size, obviously due to condition $a/Z \gg 1$ being fulfilled in such a system.

In the present paper we investigate RPs, with relatively small HFI constants (0.8−2.5 mT), formed upon the perdeuterated benzophenone photolysis in SDS micelles in the presence of 2,4,6-tri−*tert*-butylphenol. For such values of HFI constants the condition $a/Z < 1$ is realized. Taking into account the values of exchange interaction obtained previously,[4] the diminishing in SNP splitting might be expected even in relatively large SDS micelles. The influence of ESE on the SNP spectra in case of relatively small HFI constants is considered. The distinctive features of SNP in systems with natural abundance of ^{13}C nuclei are studied, and the ESE value for the corresponding RP is estimated.

There have been quite a few studies of benzophenone photolysis in SDS micelles, which is employed as a model reaction.[2,6−9] Magnetic field effects (MFE) and recombination kinetics of radical pairs formed upon photolysis of benzophenone in SDS micelles in the presence of 4-phenylphenol have been considered in detail in ref 9. The authors have evaluated the rate constants of radical escape from SDS micelles as well as the relaxation rates.

Experimental Section

A detailed description of the experimental setup for detecting SNP spectra and kinetics is described in detail elsewhere.[10] The illumination of the solution with UV light was carried out in a quartz cell positioned in a microwave cavity, which in its turn was placed in the magnetic field B_0 of an auxiliary magnet, with B_0 and the microwave field B_1 being orthogonal (resonant frequency $f_{\mathrm{res}} = 1530$ MHz). Within ca. 1 s, the sample was subsequently transferred with a flow system to the probe of a Bruker MSL-300 NMR spectrometer, where the NMR spectra of reaction products were detected. An ELI-94 excimer laser (308 nm, ca. 40 mJ per pulse, 20 Hz repetition rate) was used as a light source, and the sample illumination time was 7 s. The microwave field amplitude B_1 was checked with an inductive probe. The microwave field amplitude was calculated from the available power of the microwave source, cavity Q factor, and effective volume measured using a perturbation body method. The accuracy of evaluation of microwave amplitude was about 40%.

The experimental SNP spectrum is the magnetic field dependence of the difference in the intensities of the correspondent NMR lines in the presence of resonance microwave field B_1 and $B_1 = 0$. The essence of the time-resolved SNP technique is the introduction of a variable delay τ between the laser flash inducing the formation of RP and the edge of the microwave pulse. The SNP kinetics is the time τ dependence of the SNP signal intensity. The microwave pulse duration in

---

[†] Novosibirsk State University.

⊗ Abstract published in *Advance ACS Abstracts,* April 15, 1997.

S1089-5639(96)01544-7 CCC: $14.00

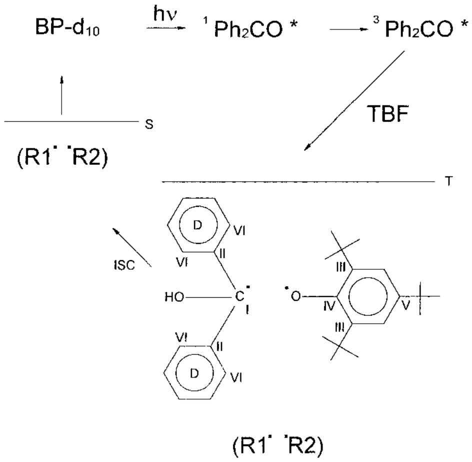

Figure 1. Reaction scheme of BP photolysis in SDS in the presence of TBP. Labels I−VI indicate the positions of ^{13}C in the respective RPs.

the experiments performed was 10 μs and the edge of microwave pulse was about 20 ns.

Perdeuterated benzophenone (BP) (Isotope, Russia) was used as received in 3 mM concentration. 2,4,6-Tri-*tert*-butylphenol (TBP) was recrystallized from hexane; its concentration was 15 mM. Sodium dodecyl sulfate (SDS) was obtained from Fluka and used as received. SDS concentration was 0.2 M. It was assumed that there can be only one radical pair per micelle.

Results and Discussion

Upon photoexcitation into the triplet state BP molecule reacts with TBP as well as with a detergent molecule.[9] In the former case a radical pair comprising a ketyl radical and a phenoxy radical (BP$^\bullet$/TBP$^\bullet$) is formed, while in the latter case BP abstracts hydrogen atom from the detergent yielding a (BP$^\bullet$/SDS$^\bullet$) pair. The laser flash-photolysis data show that with the TBP concentrations employed, the formation of the former RP takes less than 10 ns, which is much faster than what it takes for an alternative RP (BP$^\bullet$/SDS$^\bullet$) to form, τ_T ca. 300 ns.[8] We failed to observe any SNP signal upon the photolysis of BP in SDS micelles without addition of TBP. Thus the contribution of the (BP$^\bullet$/SDS$^\bullet$) pair to the experimental results is negligible, and it is not necessary to take it into account. A refined reaction scheme is shown in Figure 1.

The main reaction path after the formation of the (BP$^\bullet$/TBP$^\bullet$) pair is its recombination into starting reagents. The ^{13}C NMR spectra obtained during the photolysis of the BP and TBP in SDS micelles are shown in Figure 2, in the absence (a) and in the presence of the resonant microwave field ($B_0 = 54$ mT). Since the experiments were carried out for natural abundance of ^{13}C nuclei, spin evolution in the pairs with a magnetic nucleus in a certain position leads to polarization of this particular nucleus. We have succeeded in detecting stimulated polarization of ^{13}C nuclei for six different radical pairs, I−VI, which differ only in the position of the ^{13}C atom and hence in the HFI coupling. They are numbered in Figure 1. Each RP corresponds to its own line in the NMR (Figure 2b). The assignment of the peaks in the ^{13}C NMR spectrum is based on published data[11] for BP (I, 196.61 ppm; II, 137.49 ppm; VI, 132.33 ppm) for TBP (III, 134.82 ppm; IV, 151.24 ppm; V, 141.29 ppm). The sign of SNP polarization is given by the following relation:

$$\Gamma = \mu\epsilon\eta\nu a_k \qquad (1)$$

Here, $\mu = 1$ ($\mu = -1$) corresponds to the triplet (singlet) precursor, $\epsilon = 1$ ($\epsilon = -1$) corresponds to the incage (escape) product, a_k is the isotropic HFI constant of nucleus k, polarization for which is considered. The low-field (high-field) component of the HFI spectrum corresponds to $\eta = 1$ ($\eta = -1$); $\nu = 1$ ($\nu = -1$) when $B_1 \ll a_k$ ($B_1 \gg a_k$). $\Gamma > 0$ implies positive SNP effect (absorption); $\Gamma < 0$, negative SNP effect (emission). Apart from the ^{13}C HFI, there are only two other HFI constants in the system under study which exceed 0.1 mT: that of the hydrogens 3 and 5 of TBP ($a = 0.17$ mT) and of the OH group hydrogen of the ketyl radical ($a = 0.29$ mT),[12] for the hydrogens of BP are replaced with deuterium atoms.

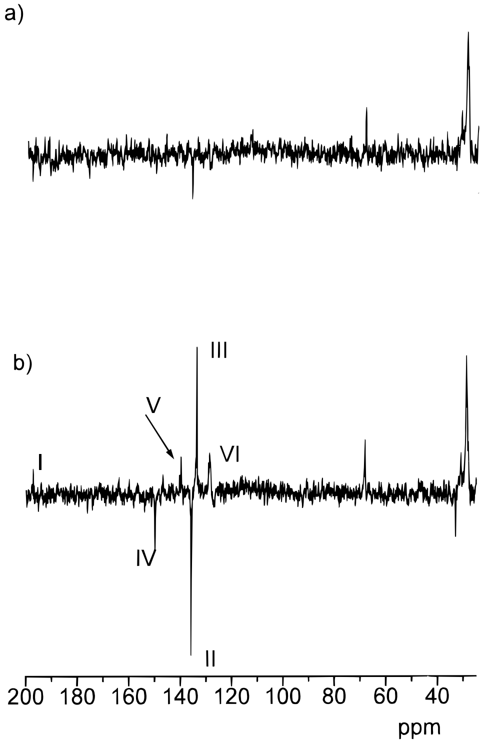

Figure 2. ^{13}C NMR spectra, obtained during the photolysis of the solution under study, acquired in the absence (a) and in the presence (b) of microwave field. $B_1 = 0.01$ mT; $B_0 = 54$ mT. Labels I−VI mark the NMR lines corresponding to the observed RPs.

The SNP spectra detected by the ^{13}C nuclei of BP and TBP (cf. Figure 1) are shown in Figures 3 and 4; they correspond to the RPs with ^{13}C nuclei in positions I (Figure 3b), III, IV (Figure 3a), and II, V (Figure 4). The sign of SNP conforms to eq 1 for in-cage product, triplet precursor RP and $a > 0$ for RPs I, III, V, and $a < 0$ for RP II, IV. Figure 5 shows the corresponding SNP kinetics obtained for RPs I ($B_0 = 53.5$ mT; $B_1 = 0.1$ mT) and II, III ($B_0 = 54.2$ mT; $B_1 = 0.01$ mT). All the kinetics obtained are single exponential, and the respective decay constants k_{obs} are given in Table 1. In the analysis of the SNP spectra and kinetics we employed a theoretical approach based on the numerical solution of the stochastic Liouville equation (SLE) within the microreactor model framework. There have been numerous successful applications of this approach to the treatment of SNP spectra and kinetics; its detailed description can be found elsewhere.[13] We have adopted the finite difference scheme proposed by Pedersen and Freed[14] and employed the Laplace transform to solve SLE. Since $a \ll B_0$, the Hamiltonian of the system was taken in high-field approximation. The exponentially decaying ESE was assumed $J(r) = J_0 \exp(-r-R_0)/\lambda$ with preexponential factor J_0 and $\lambda = 0.5$ Å. Recombination of RP in the reaction zone with thickness $\delta = 0.5$ Å was described by a dimensionless quantity, $k_s\tau$, where k_s is the recombination rate constant within the reaction zone from the singlet state, $\tau = R_0\delta/D$ is the RP residence time within

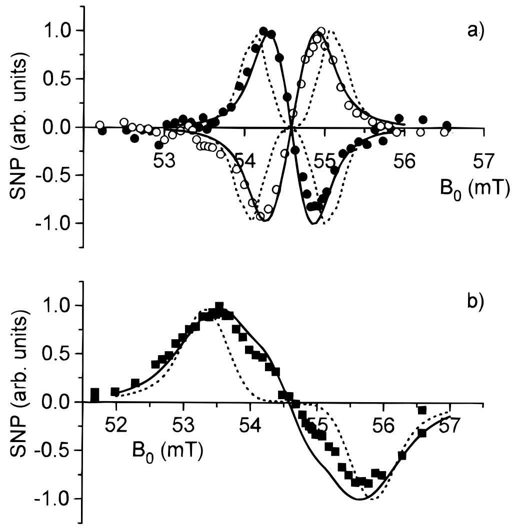

Figure 3. SNP spectra (the magnetic field dependence of the difference in the intensities of the correspondent NMR lines in the presence of resonance microwave field B_1 and $B_1 = 0$) of radical pairs IV (○), III (●); $B \approx 0.01$ mT (a) and I (■); $B_1 = 0.1$ mT. (b) Solid lines show corresponding calculated curves with $\lambda = 0.5$ Å, $J_0 = -40$ mT and HFI constants $a = -0.95$ mT (IV); $a = 0.81$ mT (III); $a = 2.5$ mT (I). Dotted lines correspond to a hypothetical spectra calculated with the same HFI constants and $J_0 = 0$.

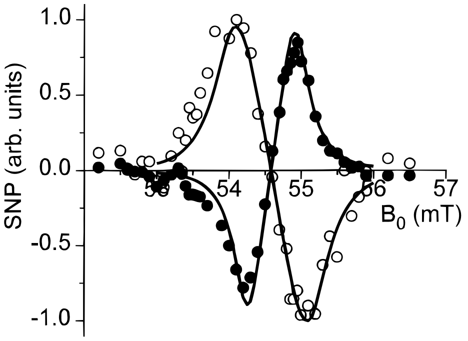

Figure 4. SNP spectra of radical pairs V (○) and II (●); $B_1 \approx 0.01$ mT. Solid lines show corresponding calculated curves with $\lambda = 0.5$ Å, $J_0 = -40$ mT and HFI constants $a = 1.3$ mT (V); $a = -0.98$ mT (II).

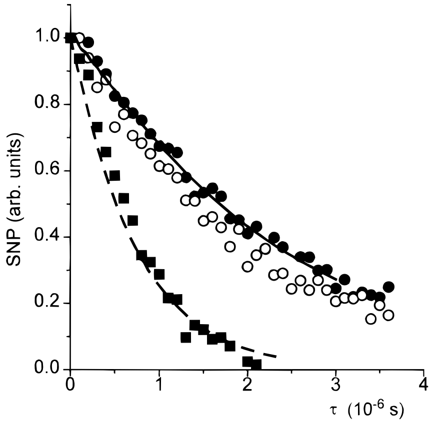

Figure 5. SNP kinetics of RP I (■, $B_0 = 53.5$ mT; $B_1 = 0.1$ mT), II (○, $B_0 = 54.1$ mT; $B_1 = 0.01$ mT), III (●, $B_0 = 54.1$ mT; $B_1 = 0.01$ mT). Solid lines show respective calculated curves.

the reaction zone, D is the mutual diffusion coefficient, and R_0 is the reaction radius. The contributions of the modulation of anisotropic HFI by diffusion (with characteristic magnitude G and rotational correlation time τ_c characterizing the spectral density of the correlation function $L(\omega) = 2G\tau_c/(1 + \omega^2\tau_c^2) = 0.5k_{rel}$) and electron dipole–dipole interaction (DDI) to the overall relaxation were treated separately. The latter contribution was treated in accord with ref 15, where the correlation function was assumed to be biexponential. The HFI values for all protons were taken from literature[12] while for deuterons of BP these values were multiplied by 0.1535. We take into account all these HFI values which caused some changes in the shape of the SNP spectra (increasing of the line width). All calculations were performed using the typical parameter values for SDS micelles,[4,16] $D = 0.8 \times 10^{-6}$ cm^2 s^{-1}; $R_m = 15.4$ Å, and $R_0 = 6$ Å for reaction radius. The slight variation of these parameters influences mainly the DDI-induced relaxation rate constant.

TABLE 1: Observed Decay Constants of SNP Kinetics k_{obs} and Relaxation Constants k_{rel} Measured for Radical Pairs I–IV with an Experimental Error of 5% (Figure 5)

radial pair	HFI coupling, mT [ref]	k_{obs}, s^{-1}	k_{rel}, s^{-1}
I	2.5 [18]	1.4×10^6	1.2×10^6
II	−0.98	4.5×10^5	2.6×10^5
III	0.81 [19]	5.1×10^5	3.2×10^5
IV	−0.95 [19]	4.5×10^5	2.6×10^5

It has been shown in ref 17 that under conditions of rapid intersystem crossing and large rate constant of decay in the reaction zone the SNP kinetics exhibits single-exponential decay with a decay parameter being the sum of the rate constants of escape and relaxation

$$k_{obs} = k_{esc} + k_{rel} \tag{2}$$

and are almost insensitive to other parameters. To evaluate k_{esc} we have studied the absorption kinetics of the BP ketyl radical (540 nm), which was detected in the flash-photolysis experiment in zero magnetic field ($B_0 = 0$) and analyzed employing the method proposed in ref 8. It is assumed that the kinetics of the ketyl radical is described by a sum of a fast exponential decay with the constant k_{decay} due to incage recombination and a slow second-order decay in the bulk. The coefficients in the relation for the time dependence of optical density

$$\mathrm{OD}(t) = \mathrm{OD}_0 + \mathrm{OD}_m \exp(-k_{decay}t) \tag{3}$$

are chosen to assure the best agreement with the experimental curve and obey the equation

$$\mathrm{OD}_0/(\mathrm{OD}_0 + \mathrm{OD}_m) = k_{esc}/(k_{esc} + k_-) \tag{4}$$

Here OD_0 is residual optical density (i.e., the “slow” component); k_- is the rate constant for all processes leading to the incage recombination of RP; and k_{esc} represents the sum of radical exit rate constants from micelle. Estimation of k_{esc} becomes straightforward when the following relation is taken into account:

$$k_{decay} = k_{esc} + k_- \tag{5}$$

Application of eqs 4 and 5 gives $k_{esc} = 1.9 \times 10^5$ s^{-1}, $k_- = 1.8 \times 10$ s^{-1}. It is necessary to note that the value obtained for the rate constant of escape is the very close to that obtained in refs 2 and 9 ($k_{esc} = 2 \times 10^5$ s^{-1}) for the (BP$^•$/SDS$^•$) pair.

Since in the case considered here the rate constants of ISC and recombination from singlet state ($k_- \gg k_{esc}$) far exceed the value of k_{rel}, the latter quantity can be determined directly from the SNP kinetics for a known value of k_{esc}. SNP kinetics for RPs I–IV (Figure 5) contain information about the relaxation of various RPs. The values of k_{obs} and k_{rel} obtained according to eq 2 with due account of k_{esc} are given in Table 1. It can be readily seen that the large anisotropy of the ^{13}C HFI in the carbonyl position as compared to that for other ^{13}C positions causes a substantial increase in k_{rel} for RP I. For this pair a limiting case of $k_{\mathrm{hfi}} \gg k_{\mathrm{ddi}}$ takes place. The corresponding theoretical curve was calculated with the following parameters: $B_0 = 53.5$ mT; $B_1 = 0.1$ mT; $a = 2.5$ mT; $k_s\tau = 0.5$; $k_{\mathrm{esc}} = 1.9 \times 10^5$ s−1; $L(\omega) = 0.5 \times 10^6$ s^{-1}. Figure 5 also demonstrates that the experimental kinetics for RPs II and III and the kinetics calculated for $B_0 = 54.1$ mT; $B_1 = 0.01$ mT; $a = 0.81$ mT ($a = -0.95$ mT); $k_s t = 0.5$; $k_{\mathrm{esc}} = 1.9 \times 10^5$ s^{-1}; $L(\omega) = 0$ (with taking into account only DDI induced relaxation) are almost identical. These kinetics is likely to be governed mainly be the radical escape from the micelle and DDI-induced relaxation and an opposite limiting case when DDI-induced relaxation predominates is realized through the small difference between kinetics II, IV, and III can be caused by difference in HFI anisotropy or τ_c. The dominate role of DDI-induced relaxation is indirectly confirmed by the results obtained in ref 9: the parameters of DDI-induced relaxation obtained there predict the value $k_{\mathrm{ddi}} = 5 \times 10^5$ s^{-1} in 54.2 mT magnetic field, which can be used as an estimate. There is another confirmation of DDI mechanism of relaxation here. We have conducted some SNP experiments during the photolysis of BP in sodium octyl sulfate micellar solution in the presence of TBP. We have not registered SNP though non-zero CIDNP have been detected. We believe it was due to fast relaxation in sodium octyl sulfate (SOS) micelles. Obviously, such an increase of the relaxation rate constant with the decrease of micelle size can be assigned with DDI-induced relaxation. Corresponding calculations show that in this case SNP intensity in SOS is in order lower than in SDS. Therefore we assume $L(\omega) = 0$ and take into account only DDI-induced relaxation in subsequent calculations. It should be noted that variation of the relative contributions of the two relaxation mechanisms while maintaining their sum invariant (k_{rel} = const) has almost no effect on the calculated SNP spectra and kinetics. Taking into account the parameters of anisotropic interaction for ^{13}C constant in RPI $A_{\|} = 5.0$ mT, $A_{\perp} < 1.5$ mT $A{:}A \geq 2.5 \times 10^{17}$ s^{-2} [18] we evaluate the correlation time of modulation of anisotropic interaction $\tau_c = 46$ ps which is in a good agreements with literature values.[4,6]

Let us now take a closer look at the SNP spectra using calculations. We note that there remain only two adjustable parameters: the magnitude of exchange interaction at the contact radius J_0 and RP recombination ability $k_s\tau$ while HFI constants a for ^{13}C nuclei in positions I ($a \approx 2.5$ mT), III ($a = 8.1$ mT), IV ($a = -0.95$ mT), V ($a = 13.9$ mT) can be found in the literature.[18,19] It is evident that the splittings in SNP spectra are noticely smaller than the values given above. It is known that the increase in J_0 or $k_s\tau$ diminishes the splitting in the SNP spectrum, since both the ESE operator and the operator describing the RP decay have the same effect upon the nondiagonal elements of the spin density matrix of the system.[20] The total rate constant of recombination from the singlet state can be estimated from the following relation

$$k_{\mathrm{rs}} = \frac{k_s\tau}{1 + k_s\tau} 4\pi R_0 D/V \tag{6}$$

where R_0 is the reaction radius, D is the coefficient of mutual diffusion of radicals within the micelle, and $V = 4\pi R_m{}^3/3$ is the micelle volume. Using the values $R_0 = 6$ Å, $R_m = 15.4$ Å, $k_{\mathrm{rs}} = 4k_- = 7.2 \times 10^6$ s^{-1}, and $D = 0.8 \times 10^{-6}$ cm^2 s^{-1} we get $k_{\mathrm{rs}} \approx 0.2 \times 4\pi R_0 D/V$, i.e., the reaction is likely to be not diffusion controlled and $k_s\tau < 1$. Using the relation $k_s\tau/(1 + k_s\tau) \approx 0.2$ we get $k_s\tau \approx 0.3$. This is only an estimate, but we can conclude that the real value of $k_s\tau$ should be higher than 0.3 since this estimation implies fast ISC in zero field but the value taken from ref 7, 4.0×10^6 s^{-1}, is comparable with k_{rs}. The variation of $k_s\tau$ over a wide range of values, $0.03 < k_s\tau < 2$, has almost no effect on the calculated kinetics for RP I. Calculated SNP kinetics for other RPs and SNP spectra for all RPs are insensitive to the variation of $k_s\tau$ even in wider range. Therefore, we set $k_s\tau = 0.5$ and will only vary the value of J_0.

Numerical calculations for pairs III and IV show (Figure 3) that in the absence of exchange interaction the splitting in SNP spectrum is noticely larger than experimentally observed one. The decrease in the splitting for the calculated spectrum can be attained when the value $|J_0| > 20$ mT is used. From the comparison of the calculated spectra with the experimental ones, it is possible to estimate its value as $|J_0| > 40$ mT, which leads to necessary dminishing of the observed splitting in a spectrum. The further increasing of $|J_0|$ does not lead to any changes in the spectra. Note that this diminishing is compensated by the increasing of the line width and calculations without relaxation and additional nuclei show the decrease in the splitting to approximately half of the HFI value. The comparison of the calculated SNP spectrum for RP I with the experimental one confirms the same estimate for the lower limit of $|J_0|$ values though due to relatively high HFI value and line width the diminishing is not so noticeable. In case of RP I the value $|J_0| = 40$ mT also provides the correct line width. Note that the fitted parameters for the exchange interaction are J_0 and λ. It is clear that these two parameters are connected with each other and the increasing of λ leads to the decreasing of J_0 and vice versa. The increasing of the parameter λ to 1 Å leads to the slight decreasing of the estimation of exchange interaction $|J_0| > 30$ mT.

It is remarkable that our estimation of J_0 is also in good agreement with the value $J_0 = -60$ mT obtained in previous simulations of SNP spectra for different RPs.[21] We note that the reduced splitting in an SNP spectrum as compared to the full HFI constant has never been observed in SDS micelles before, for the systems with large HFI constants were commonly studied.[4] Using the obtained parameters of exchange interaction we simulate the SNP spectra and evaluate the value of HFI constants in positions II and V (Figure 4). The ^{13}C HFI constant for RP II has been evaluated by the comparison of the experimental and calculated spectra and is given in Table 1.

Conclusion

In the present study the ^{13}C-stimulated nuclear polarization (SNP) technique has been applied to study perdeuterated benzophenone in SDS micelles in the presence of 2,4,6-tri-*tert*-butylphenol at a natural abundance of ^{13}C. The SNP spectra and kinetics have been detected for radical pairs differing in the position of ^{13}C atom. Except for the HFI constant, such pairs have identical parameters, which provides an opportunity to study the effect of the HFI constant upon the relaxation and recombination processes in RPs. It has been shown that the main relaxation mechanism which governs the kinetics decay for RP I with ^{13}C nucleus in carbonyl position is the modulation of HFI anisotropy.

The experimental spectra obtained have been simulated within the framework of the numerical solution of the stochastic Liouville equation as applied to the microreactor model. A lower limit for the electron exchange interaction constant has been estimated as $|J_0| > 40$ mT. ESE leads to a decrease in the splitting in SNP spectra of the RP under study.

Acknowledgment. The authors are grateful to Dr. Valery Tarasov for fruitful discussions and Dr. Yu. Tsentalovich for his help in flash-photolysis measurements. This work is kindly supported by INTAS (Grant No. 93-1626) and the Russian Foundation of Basic Research (Grant No. 96-03-32930).

References and Notes

(1) Batchelor, S. N.; McLauchlan, K. A.; Shkrob, I. A. *Mol. Phys.* **1992**, *75*, 531.

(2) Okazaki, M.; Toriyama, K. *Bull. Chem. Soc. Jpn.* **1993**, *66*, 1892. Polyakov, N. E.; Konishi, Y.; Okazaki, M.; Toriyama, K. *J. Phys. Chem.* **1994**, *98*, 10558. Polyakov, N. E.; Okazaki, M.; Toriyama, K.; Leshina, T. V.; Fujiwara, Y.; Tanimoto, Y. *J. Phys. Chem.* **1994**, *98*, 10563.

(3) Bagryanskaya, E. G.; Sagdeev, R. Z. *Prog. React. Kinet.* **1993**, *18*, 63.

(4) Tarasov, V. F.; Bagryanskaya, E. G.; Shkrob, I. A.; Avdievich, N. I.; Ghatlia, N. D.; Lukzen, N. N.; Turro, N. J.; Sagdeev, R. Z. *J. Am. Chem. Soc.* **1995**, *117*, 110.

(5) Ananchenko, G. S.; Bagryanskaya, E. G.; Tarasov, V. F.; Sagdeev, R. Z.; Paul, H. *Chem. Phys. Lett.* **1996**, *255*, 267.

(6) Yoshida, H.; Warashina, T. *Bull. Chem. Soc. Jpn.* **1971**, *44*, 2950.

(7) Hayashi, H.; Nagakura, S. *Bull. Chem. Soc. Jpn.* **1984**, *57*, 322. Sakagushi, Y.; Hayashi, H.; Nagakura, S. *J. Phys. Chem.* **1982**, *86*, 3177.

(8) Evans, C. H.; Ingold, K. U.; Scaiano, J. C. *J. Phys. Chem.* **1988**, *92*, 1257. Evans, C. H.; Scaiano, J. C.; Ingold, K. U. *J. Am. Chem. Soc.* **1992**, *114*, 140.

(9) Levin, P. P.; Safirovich, V. Ya.; Kuzmin, V. A. *J. Phys. Chem.* **1992**, *96*, 10044.

(10) Avdievich, N. I.; Bagryanskaya, E. G.; Grishin, Yu. A.; Sagdeev, R. Z. *Chem. Phys. Lett.* **1989**, *155*, 141.

(11) Pouchert, C. J.; Behnke, J. *The Aldrich Library ^{13}C and ^{1}H FT NMR spectra*, 1st ed.; Aldrich: Milwaukee, WI, 1993; Vol. 2.

(12) Fischer, H., Hellwedge, K. H., Eds. *Landolt-Bornstein, New Series, Group 2*, Springer: Berlin, 1977; Vol. 9.

(13) Parnachev, A. P.; Bagryanskaya, E. G.; Tarasov, V. F.; Lukzen, N. N.; Sagdeev, R. *Chem. Phys. Lett.* **1995**, *244*, 245. Shkrob, I. A.; Tarasov, V. F.; Bagryanskaya, E. G. *Chem. Phys.* **1991**, *153*, 427.

(14) Pedersen, J. B.; Freed, J. H. *J. Chem. Phys.* **1991**, *61*, 1517. Zientara, G. P.; Freed, J. H. *J. Chem. Phys.* **1979**, *70*, 1359.

(15) Steiner, U. E.; Wu, J. Q. *Chem. Phys.* **1992**, *162*, 53.

(16) Tarasov, V. F.; Ghatlia, N. D.; Avdievich, N. I.; Shkrob, I. A.; Buchachenko, A. L.; Turro, N. J. *J. Am. Chem. Soc.* **1994**, *116*, 2281.

(17) Avdievich, N. I.; Bagryanskaya, E. G.; Tarasov, V. F.; Sagdeev, R. Z. *Z. Phys. Chem.* **1993**, *182*, 107.

(18) Nakagaki, R.; Takahira, O.; Hiruta, K. *Chem. Phys. Lett.* **1995**, *233*, 41. Falle, H. R.; Adam, F. C. *Can. J. Chem.* **1966**, *44*, 1387.

(19) Kirste, B. *J. Magn. Reson.* **1985**, *62*, 242.

(20) Shushin, A. I. *Chem. Phys. Lett.* **1991**, *181*, 274. Koptyug, I. V.; Lukzen, N. N.; Bagryanskaya, E. G.; Doktorov, A. B. *Chem. Phys. Lett.* **1990**, *175*, 467.

(21) Bagryanskaya, E. G.; Sagdeev, R. Z. *Z. Phys. Chem.* **1993**, *180*, 111. Bagryanskaya, E. G.; Tarasov, V. F.; Avdievich, N. I.; Shkrob, I. A. *Chem. Phys.* **1992**, *162*, 213.